



ANNUAL
REVIEWS **Further**

Click [here](#) for quick links to Annual Reviews content online, including:

- Other articles in this volume
- Top cited articles
- Top downloaded articles
- Our comprehensive search

Ion Chemistry in the Interstellar Medium

Theodore P. Snow and Veronica M. Bierbaum

Center for Astrophysics and Space Astronomy, Department of Astrophysical and Planetary Sciences and Department of Chemistry and Biochemistry, University of Colorado, Boulder, Colorado 80309; email: Theodore.Snow@colorado.edu, Veronica.Bierbaum@colorado.edu

Annu. Rev. Anal. Chem. 2008. 1:229–59

The *Annual Review of Analytical Chemistry* is online at anchem.annualreviews.org

This article's doi:
10.1146/annurev.anchem.1.031207.112907

Copyright © 2008 by Annual Reviews.
All rights reserved

1936-1327/08/0719-0229\$20.00

Key Words

ion-atom reactions, interstellar clouds, interstellar species

Abstract

We present an overview of the interstellar medium, including physical and chemical conditions, spectroscopic observations, and current challenges in characterizing interstellar chemistry. Laboratory studies of ion-atom reactions, including experimental approaches and instrumentation, are described. We also tabulate and discuss comprehensive summaries of ion-neutral reactions involving hydrogen, nitrogen, and oxygen atoms that have been studied since Sablier and Rolando's 1993 review.

ISM: interstellar medium

1. INTRODUCTION TO THE INTERSTELLAR MEDIUM

The physical conditions of the interstellar medium (ISM) are unlike any that occur naturally on Earth, and they are extremely difficult to reproduce in laboratory experiments. The ISM particle densities in our galaxy range from 10^{-4} cm^{-3} in diffuse regions to 10^5 cm^{-3} in dense clouds, the latter comparable to the best laboratory vacuums. Temperatures in these regions range from 10 K to 150 K. But, strange as it may seem, an active chemistry converts these atoms to molecules, some large and complex.

Despite the harsh, seemingly unproductive conditions in the ISM, two aspects of astrochemistry emerge as critical. One is that ions, formed by particle collisions, intense UV starlight, and cosmic rays, have high ion-neutral reaction rates. The other pertains to the timescales over which reactions can proceed. In a typical diffuse interstellar cloud, the average time between particle collisions is measured in decades—but cloud lifetimes can be millions of years. In denser interstellar clouds, collision times are reduced to a few hours.

Laboratory experiments are a valid means of exploring the chemistry of the ISM because steady-state conditions can be achieved and pressure and temperature effects are generally understood. The relevant reactions are two-body processes with no activation barrier; the neutral partner has a dipole moment that either occurs naturally or is induced by the ionic collision partner, so there is an attractive force between the particles. The frequency of reactive collisions can be determined by cloud densities and reaction rate constants. Unfortunately, most rate constants have been measured at room temperature, not at the very cold temperatures of interstellar space. However, temperature-variable experiments have often demonstrated either a simple temperature dependence or no dependence at all.

Evidence that a rich chemistry does operate in the ISM (1, 2) has been found in the observations of ~ 140 molecules to date (**Table 1**). There is evidence for the existence of far larger molecular species, the identities of which currently elude investigators. Laboratory results enable theorists to construct accurate chemical models of these clouds. These models refine the calculated abundances of observed species and make predictions about other species not yet observed.

Because this review is intended for a general scientific audience, we first give an overview of the physical and chemical conditions in the interstellar medium, then address several major challenges in astrochemistry that can be explored in the laboratory.

1.1. Physical and Chemical Conditions in the Interstellar Medium

The ISM is extremely heterogeneous. Instead of a rarefied, uniform environment, astronomers find a patchy, clumpy medium with extremes of temperature and a broad range of densities. **Table 2** presents physical data characteristic of the various regimes in interstellar clouds, derived from observations made throughout the electromagnetic spectrum using ground- and space-based telescopes.

1.1.1. Observations. The ISM was first detected by astronomers who observed that the Milky Way is punctuated by dark clouds (**Figure 1**). The interstellar dust is visible, and dark clouds obscure the stars within and behind these regions. The interstellar gas

Table 1 Detected interstellar molecules^{a,b}

H ₂ ^{c,d}	CF ⁺	SiCN	C ₄ H ⁻	CH ₃ NH ₂
AlF	C ₃ ^{e,f}	AlNC	HC ₂ NC	c-C ₂ H ₄ O
AlCl	C ₂ H	SiNC	HCOOH	H ₂ CCHOH
C ₂ ^{d,e}	C ₂ O	HCP	H ₂ CNH	CH ₂ CHCN
CH ^e	C ₂ S	c-C ₃ H	H ₂ C ₂ O	CH ₃ C ₃ N
CH ⁺ ^e	CH ₂ ^{d,f}	<i>l</i> -C ₃ H	H ₂ NCN	HC(O)OCH ₃
CN ^e	HCN ^{f,g}	C ₃ N	HNC ₃	CH ₃ COOH
CO ^{c,d,f}	HCO	C ₃ O	SiH ₄	C ₇ H
CO ⁺	HCO ⁺	C ₃ S	H ₂ COH ⁺	H ₂ C ₆
CP	HCS ⁺	C ₂ H ₂ ^c	HC ₃ N	CH ₂ OHCHO
SiC	HOC ⁺	NH ₃	C ₅ H	CH ₂ CCHCN
HC1 ^d	H ₂ O	HCCN	<i>l</i> -H ₂ C ₄	CH ₃ C ₄ H
KCl	H ₂ S	HCNH ⁺	C ₂ H ₄	CH ₃ CH ₂ CN
NH ^e	HNC	HNCO	CH ₃ CN	(CH ₃) ₂ O
NO	HNO	HNCS	CH ₃ NC	CH ₃ CH ₂ OH
NS	MgCN	HOCO ⁺	CH ₃ OH	HC ₇ N
NaCl	MgNC	H ₂ CO	CH ₃ SH	CH ₃ C(O)NH ₂
OH ^{d,f}	N ₂ H ⁺	H ₂ CN	HC ₃ NH ⁺	C ₈ H
PN	N ₂ O	H ₂ CS	HC ₂ CHO	C ₈ H ⁻
SO	NaCN	H ₃ O ⁺	NH ₂ CHO	CH ₃ C ₅ N
SO ⁺	OCS	c-SiC ₃	C ₅ N	(CH ₃) ₂ CO
SiN	SO ₂	CH ₃ ^c	<i>l</i> -HC ₄ N	(CH ₂ OH) ₂
SiO	c-SiC ₂	C ₅	c-H ₂ C ₃ O	CH ₃ CH ₂ CHO
SiS	CO ₂ ^c	C ₄ H	C ₆ H	HC ₉ N
CS	NH ₂ ^c	<i>l</i> -C ₃ H ₂	C ₆ H ⁻	CH ₃ C ₆ H
HF ^{c,f}	H ₃ ⁺ ^c	c-C ₃ H ₂	CH ₃ C ₂ H	HC ₁₁ N
SH	H ₂ D ⁺	H ₂ CCN	HC ₅ N	
O ₂ ^g	HD ₂ ⁺	CH ₄	CH ₃ CHO	

Annotations:

^a Most of this information was gathered from Reference 13. Many of these species have detected isotopologues, which are not listed. Additional detections that are questionable or probable include N₂, FeO, SiH, *l*-HC₄H, H₂CCNH, *l*-HC₆H, CH₂CHCHO, C₆H₆, C₂H₅OCH₃, H₂NCH₂COOH (glycine), and 1,3-dihydroxypropanone.

^b Molecules without annotations have been detected only by rotational transitions in the radiofrequency spectrum.

^c Detected by vibrational transitions in the infrared region.

^d Detected by electronic transitions in the UV region.

^e Detected by electronic transitions in the visible region.

^f Detected by rotational transitions in the radiofrequency spectrum, as well as another method or methods, as specified.

^g Detected by rotational transitions at submillimeter wavelengths.

is visually evident only when it is hot and glowing (the reddish regions of **Figure 1**); spectroscopic observations are usually needed to explore the properties of the gas.

On its journey to us, starlight is selectively absorbed by atoms, ions, and molecules in interstellar space. There are few absorption lines at visible wavelengths because only transitions arising from the ground electronic state are seen, and these occur

Table 2 Physical conditions in molecule-bearing interstellar clouds^{a,b}

Property	Cloud type			
	Diffuse atomic	Diffuse molecular	Translucent	Dense molecular
Defining characteristic	$f_{\text{H}_2}^{\text{n}} < 0.1$	$f_{\text{H}_2}^{\text{n}} > 0.1$ $f_{\text{C}^+}^{\text{n}} > 0.5$	$f_{\text{CO}}^{\text{n}} < 0.9$ $f_{\text{C}^+}^{\text{n}} < 0.5$	$f_{\text{CO}}^{\text{n}} > 0.9$
A_V (minimum)	0–0.2	~0.2–1	~1–5	~5–10
Typical n_{H} (cm^{-3})	1–100	100–500	500–5000	10^4 – 10^6
Typical T (K)	30–150	30–100	15–50	10–50
Observational techniques	UV/visible absorption, H I radio emission	UV/visible/IR absorption, radio absorption	Visible/UV, IR absorption, radio absorption/emission	IR absorption, radio emission

^aAbbreviations: $f_{\text{H}_2}^{\text{n}}$, the fraction of hydrogen nuclei contained in the form of H_2 ; $f_{\text{H}_2}^{\text{n}} = 2\text{N}(\text{H}_2)/[\text{N}(\text{H}) + 2\text{N}(\text{H}_2)]$, where the N symbolizes column density, which is the product of the volume density and the path length between Earth and the observed star; $f_{\text{C}^+}^{\text{n}}$ and f_{CO}^{n} , the ionized carbon or CO molecular fraction, as compared to the total hydrogen, using observed column densities; A_V , the dust extinction parameter, a logarithmic value expressed in units of stellar magnitudes, refers to the extinction at visual wavelengths; n_{H} , the volume density of hydrogen nuclei, which is usually inferred by indirect means; H I, the astronomical term for H-atom; IR, infrared.

^bBased on table 1 in Reference 26.

mostly in the UV region. The density, and therefore the collision rate, is too low to maintain populations in excited electronic states. Typically, in the visible region, interstellar atomic lines are observed for Na (the D lines), K, Fe, and Ca, and for some ions, such as Ca^+ (the H and K lines). About 70 years ago, three molecules were identified in visible-wavelength spectra: CH, CH^+ , and CN (3–6). These observations led to the first discussions concerning how molecules could form in the low-density environment of interstellar space; ion-neutral reactions were proposed as efficient mechanisms (7–9). For a review of this topic, see Dalgarno (10).

Because most electronic transitions arising from the ground state of atoms, ions, and molecules occur at UV wavelengths, most interstellar absorption lines can only be observed from telescopes above the Earth's atmosphere. There have been many orbiting space-based observatories that obtain UV spectra, culminating with the Hubble Space Telescope. With these telescopes, most common elements (except helium) can be observed in either neutral atomic or ionic form. Moreover, the most abundant molecules in space, such as H_2 and CO, have absorption lines in the UV and are easily observed, at least in diffuse clouds where UV radiation can penetrate. A typical UV spectrum, including both atomic and H_2 lines, is shown in **Figure 2**.

A new means of observing interstellar molecules was developed in the 1960s, when the first rotational emission lines were detected at millimeter wavelengths (11, 12). Despite the low gas densities, occasional collisions—especially in denser clouds—have enough energy and frequency to maintain a population of rotationally excited molecules. Only molecules that have a nonzero dipole moment can be detected through millimeter-wave emission lines when the rotationally excited molecules cascade down to the ground state. Homonuclear molecules, such as H_2 and C_2 , have no dipole moment and no rotational (or vibrational) transitions, and can be observed only through their electronic dipole transitions or through forbidden (quadrupole) vibrational transitions. About 140 molecules have now been detected through their



Figure 1

The interstellar medium. This CCD image, taken by Adam Block at the Caelum Observatory, shows many aspects of the interstellar medium, including dark clouds, ionized hydrogen regions (known as H II regions due to H- α emission) (*red*), a newly-formed star cluster (*lower center*), nebulae caused by light scattered from dust grains (*blue*), and stars (*reddish color*) seen through the interstellar dust. Most molecules identified by their radio emission lines are found in the dark clouds; however, some are found in more diffuse regions through optical and UV absorption along the lines of sight toward reddened stars. Copyright Adam Block and Tim Puckett. Reproduced with permission.

radio emission lines, from diatomics to polyynes with 13 atoms (**Table 1**) (13). The vast majority of the detected species contains carbon. Although no biological molecules have been conclusively detected, the search for simple amino acids is ongoing and shows some promise (14); however, the one reported detection is probably not valid (15).

Until recently, only neutral and singly charged positive ions had been found, but there have now been exciting discoveries of several negative ions (16–18). These anions may be important in forming some interstellar neutrals through ion chemistry; however, studies of such mechanisms are in their infancy. To date, the largest unambiguously identified interstellar molecules contain carbon chains, but there are

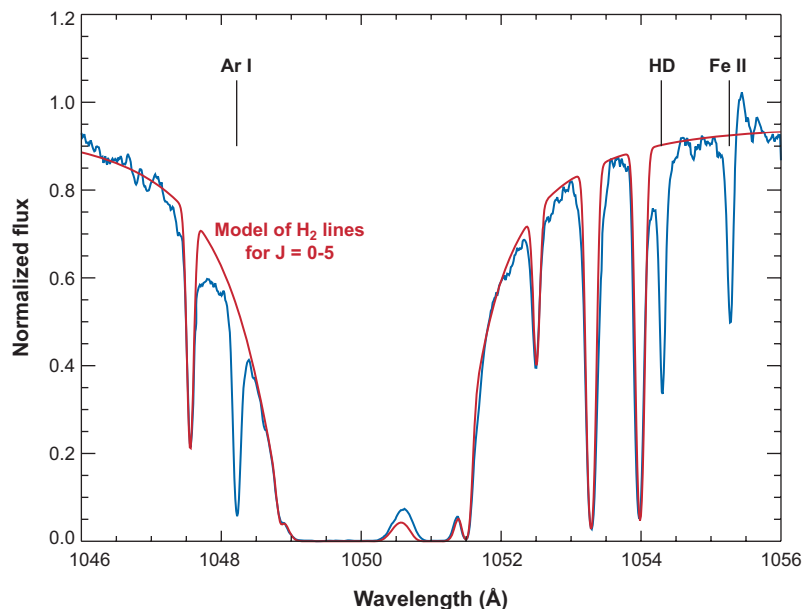


Figure 2

UV spectrum showing interstellar absorption lines obtained by NASA's Far Ultraviolet Spectroscopic Explorer. In this image, most of the line absorption features are due to interstellar H_2 molecules, two lines are the result of interstellar atoms and ions, and one line represents interstellar HD molecules. The smooth profile is a fit to the H_2 band, with rotational levels from $J = 0$ to $J = 5$. Both the H_2 and HD features are due to transitions from the ground electronic and vibrational states, but some excitation to low-lying rotational states is evident. Abbreviations: Ar I, neutral form of argon; Fe II, singly ionized form of iron. Copyright NASA and the Center for Astrophysics and Space Astronomy, University of Colorado. Reproduced with permission.

hints that much larger species exist. Interstellar polycyclic aromatic hydrocarbons (PAHs) are almost certainly present, as shown by their infrared (IR) emission bands (19–21).

IR emission and absorption constitute another spectral window for observing interstellar molecules; the observed lines are predominantly the result of transitions between vibrational levels. Only in irradiated, relatively dense regions (known as photon-dominated regions or PDRs) are vibrational lines seen in emission. Interestingly, H_2 , which has no allowed vibrational transitions, is seen in emission in PDRs through low-probability quadrupole transitions (22, 23); this detection is possible because of the high abundance of H_2 .

A few IR interstellar absorption lines from gas-phase species are observed, usually from the ground- and vibrationally excited levels of the ground electronic state. Despite its high abundance, H_2 is rarely seen in IR absorption (24); however, CO, which has allowed vibrational transitions and is second in abundance among interstellar molecules, is observed in absorption (25).

PAH: polycyclic aromatic hydrocarbon

PDR: photon-dominated region

1.1.2. Physical conditions. As already noted, the ISM is heterogeneous, with relatively dense clouds or nebulae that account for most of its mass. At the other extreme, the intercloud medium has extremely low densities and occupies most of the volume of the galaxy. The dense molecular clouds are often components of large aggregates containing many hundreds of solar masses. These complexes, such as those seen in **Figure 1**, are the birthplaces of new stars. **Table 2** summarizes the conditions in these clouds, where the temperatures can be as low as 15–20 K and the densities as high as 10^5 – 10^6 cm $^{-3}$.

The dense clouds are largely molecular in nature and are composed primarily of H $_2$ followed by CO, which constitutes about 10^{-4} of the abundance of H $_2$ by number. Other simple species such as OH, CH, CN, and H $_2$ O represent only 10^{-7} of the abundance of H $_2$, at most. The density of PAHs in the general ISM is unknown, but some astronomers estimate the abundance as comparable to the simple species mentioned above, thus accounting for 15 to 20% of the carbon in the ISM (19–21).

Both translucent and diffuse molecular clouds (**Table 2**) have molecular populations. **Figure 3** illustrates several types of clouds. Although the sequence is not necessarily evolutionary, one can imagine a set of conditions smoothly changing from

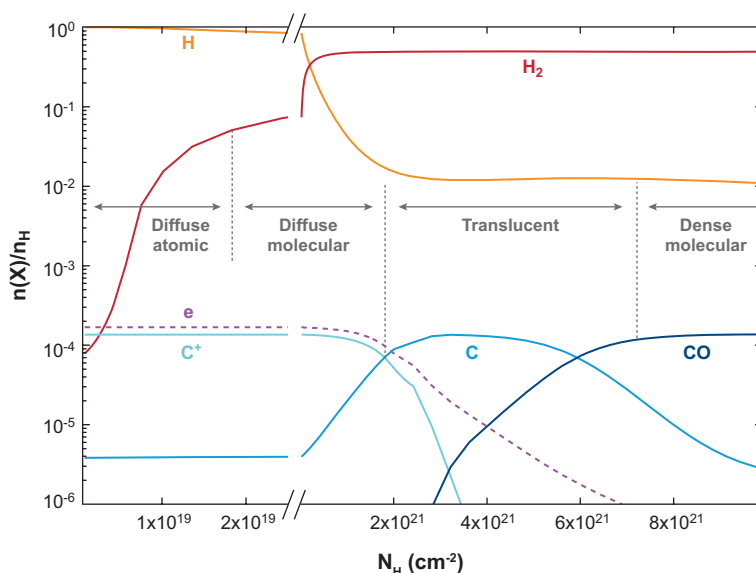


Figure 3

Physical and chemical conditions in interstellar clouds. The ordinate specifies the density of the given species relative to total hydrogen; the abscissa indicates the total hydrogen column density (the product of the hydrogen volume density and the path length). Moving from the diffuse atomic clouds (*left*) to the dense molecular clouds (*right*), there are major transitions of the dominant atoms, ions, and molecules. Molecules in the dense molecular and translucent clouds can be observed by radio-wave emission lines, and some molecules (such as CO) can be detected by the same method in diffuse molecular clouds. In diffuse atomic and molecular clouds, the interstellar species are primarily observed through absorption lines at visible or UV wavelengths. Reproduced with permission from Reference 26.

diffuse atomic to dense molecular clouds. **Figure 3** and **Table 2** indicate that diffuse atomic clouds contain mostly atomic hydrogen and ionic species, with a molecular fraction (i.e., H_2 as compared by number to all hydrogen nuclei) of 0.0 to 0.1. For diffuse molecular clouds, the molecular hydrogen fraction lies between 0.1 and ~ 0.5 , and increases to nearly 1.0 in translucent and dense molecular clouds. The distinction between these latter clouds relates to the form of carbon: In translucent clouds, carbon exists as the ionized or neutral atomic form with the CO fraction beginning to rise. In dense molecular clouds, all of the hydrogen and most of the carbon are in molecular form.

The main factors that determine the physical and chemical conditions in the various cloud types are density, temperature, and the radiation field. The density is controlled by gas motions caused by random perturbations, stellar winds, and stellar explosions such as supernovae (the ISM is a violent environment!). The temperatures in the various regimes are determined by heat input, which depends upon radiation and kinetics of the gas, and heat losses, which primarily depend upon radiative losses from excited states of atoms, ions, and molecules.

The intensity of the radiation field is driven by the field's proximity to hot stars and the attenuation (i.e., extinction) of starlight by dust. When very close to a hot star, molecules can still form despite the high intensity of the radiation field as long as the density is sufficiently high (high density may result from shocks compressing the gas). Interstellar dust further away from hot stars causes wavelength-dependent extinction (**Figure 4**), which greatly affects the ambient radiation field and hence the molecular

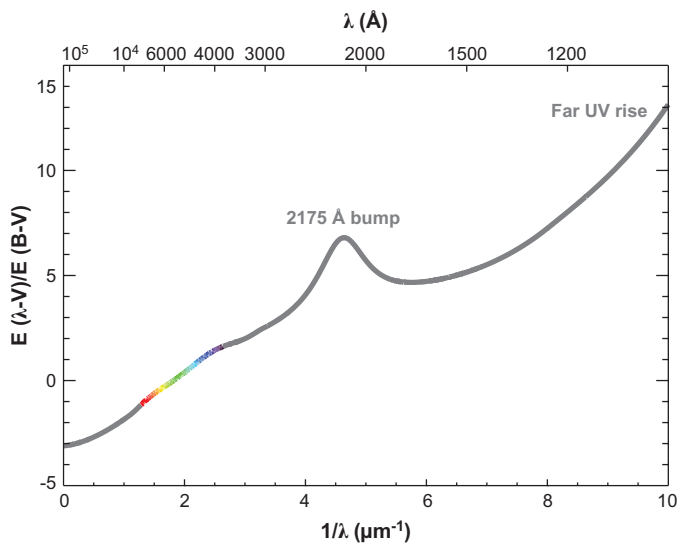


Figure 4

The UV interstellar dust extinction curve. The effect of interstellar dust in blocking starlight rises toward short wavelengths; therefore, in the UV portion of the spectrum—where the majority of interstellar atoms, ions, and molecules have electronic transitions—it is difficult to observe the interstellar absorption lines. The prominent “bump” centered at 2175 Å is thought to be caused by carbonaceous dust or perhaps by polycyclic aromatic hydrocarbons.

population. As **Figure 4** shows, the extinction rises toward UV wavelengths, so the effect of dust is greatest in the spectral window where molecules are mostly likely to be either dissociated or prevented from forming. As shown in **Table 2**, dust extinction (denoted by A_V , a logarithmic value) is a critical factor that varies with cloud type.

1.1.3. Chemical modeling of interstellar clouds. A complete chemical model of an interstellar cloud should include the physical and chemical conditions described above, namely (*a*) the gas kinetics; (*b*) the depth-dependence of density and temperature from the exterior to the interior of the cloud; (*c*) the time variability as the cloud evolves; and (*d*) the correct reaction rates. These are demanding criteria, and no complete model has been developed, although progress is being made. See Snow & McCall (26) for a recent summary of chemical modeling.

1.2. Current Challenges

We identify several problems in constructing better models and gaining more insight into the chemistry of the ISM. In this section, we outline some of those challenges.

1.2.1. The interdependence of related reactions. A stable population of a given molecular species is maintained through the combination of formation and destruction processes. As many abundant species are formed through a sequence of steps, the rate constants of many intermediate processes can be important; however, many of these rate constants are poorly understood, if at all.

Recently, Markwick-Kemper compiled a list of the most important reactions, ranked by potential impact due to uncertainties in the rate constants (27). Some of the most abundant species have been shown to have uncertainties in their theoretical abundances of 50% or greater; these uncertainties can be propagated through the network of sequential reactions. Wakelam et al. (28) have recently considered the effect of uncertainties on the chemical models of dark clouds.

There are at least two major databases of reaction rate constants that are relevant to ISM chemistry models: One database is maintained by Woodall et al. (29) and the other by Herbst (30). There is occasional disagreement between these databases, which highlights uncertainties and identifies the rate constants that should be re-examined.

1.2.2. The formation and abundance of molecular anions. The first molecular anions (C_4H^- , C_6H^- , and C_8H^-) have recently been detected (16–18) in interstellar space and circumstellar envelopes (i.e., shells or bubbles of gas ejected by stellar winds). Observations of other carbon chain anions are anticipated. Millar et al. (31), using the code for PDRs proposed by Le Petit et al. (32), have calculated that $C_{10}H^-$ should be comparable in abundance to C_6H^- and C_8H^- ($\sim 10^{-9}$ of the total particle number density). As the length of the carbon chain increases, the abundance is expected to diminish only slowly; thus, even larger anions could potentially be observed.

Negative molecular ions, in addition to being sufficiently abundant for detection in space, can play a crucial role in ion chemistry. Our work has shown that some observed

DIB: diffuse interstellar band

interstellar neutrals can be formed by reactions involving anions as reagents. These reaction sequences can form, for example, cyanoacetylene and glycine, the simplest amino acid (33). Positive ion gas-phase syntheses for interstellar carboxylic and amino acids have been proposed by Bohme and colleagues (34).

1.2.3. The search for biological molecules. A new field of astrochemistry, known variously as bioastronomy or astrobiology, has been born. Astrobiology has generated new courses, conferences, faculty lines, and institutes (e.g., the Search for Extraterrestrial Intelligence Institute), as well as funding from the National Aeronautics and Space Administration. Although no sign of extraterrestrial life has been found to date, many scientists remain optimistic.

One step toward the discovery of extraterrestrial life would be the positive detection of biological molecules in interstellar space. As noted above, mechanisms for producing simple amino acids in interstellar clouds have been found to be feasible, and there has been a reported (14) but contested (15) detection of interstellar glycine. However, models based on experimental work predict that glycine, and perhaps other biogenic molecules, should be sufficiently abundant for detection. Such discoveries could yield insights into the origin of life.

1.2.4. The diffuse interstellar bands. Diffuse interstellar bands (DIBs) have a long history, having first been reported in 1922 (35). DIBs consist of a set of absorption features (**Figure 5**), are definitely interstellar, and are almost certainly caused by

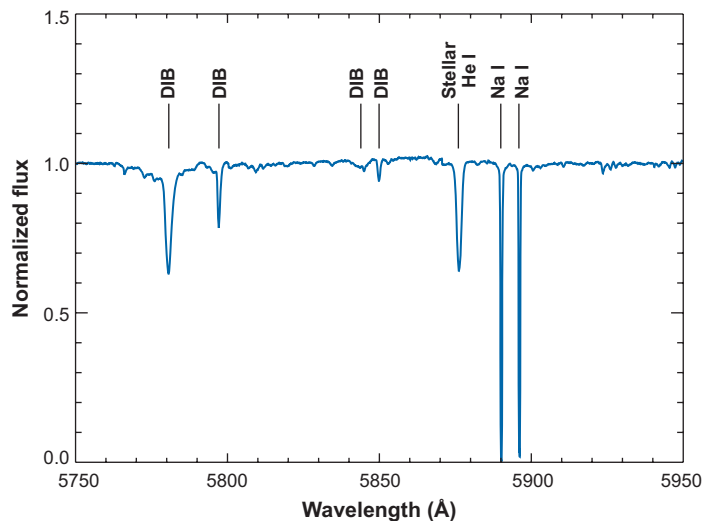


Figure 5

Diffuse interstellar bands (DIBs). This figure shows four broad, weak features that are part of the 300+ DIBs. At right are the interstellar sodium D-lines and one stellar line (He I represents helium in its neutral state). The two DIBs toward the left end of the spectrum are those first noticed more than 85 years ago (35). Data from the 3.5-m telescope at Apache Point, New Mexico, operated and owned by Astronomical Research Corporation. Used with permission.

large organic molecules (36, 37). The identity of the DIB carriers is the oldest astronomical spectroscopic mystery by far. After decades of being ignored or viewed as a fringe problem, beginning in the 1980s DIBs have been recognized by astronomers as holding the key to numerous issues in ISM chemistry.

Based on observational properties and the probable presence of PAHs in the ISM, along with experimental data and physical models of the ionization state of interstellar PAHs (38, 39), PAH cations have emerged as very strong candidates for DIB carriers. Carbon chains are also considered candidates as they comprise the majority of identified interstellar molecules (see **Table 1**). However, carbon chains have not yet been detected in diffuse atomic clouds in which DIBs are strongest.

The models and experiments point to PAH cations having 30 or more carbon atoms as the most likely DIB carriers (39). However, such large PAHs present difficulties to kineticists and spectroscopists as they are difficult to vaporize and retain in the gas phase as cations. From solid-state spectroscopy, we know that PAH cations having 30 or more carbon atoms have strong spectra at visible wavelengths and that neutral PAHs tend to have their lines and bands in the UV; however, only gas-phase spectroscopy can identify the specific species responsible for the DIBs.

Estimates of the PAH abundance in the ISM suggest that 15–20% of the entire galactic ISM carbon budget could exist in this form (19–21); this abundance would be sufficient to account for the observed absorption of starlight through DIBs. Whatever molecules are responsible for DIBs, their identification will yield new insights into the chemistry of the ISM. It will reveal their role in the energy budget of the ISM and in the formation of other species, possibly including biogenic molecules. Great acclaim surely awaits the scientists who finally identify the DIB carriers, and lab work will play a major role in that eventual success.

1.2.5. Identifying polycyclic aromatic hydrocarbons in the interstellar medium.

In addition to the DIB problem, the PAHs themselves represent a challenge to ISM chemists. The infrared emission bands associated with PAHs arise from vibrational transitions (such as C-C or C-H stretching or bending modes), which are relatively similar for most PAH molecules (19–21). However, the electronic spectra are unique; therefore, if the electronic spectra of PAHs or their cations were known, astronomers could search for specific molecules, perhaps even those responsible for DIBs. More relevant to this review, laboratory studies of reaction rates with appropriate modeling can identify PAHs for spectroscopic study, which in turn can enable identification of PAHs in the ISM.

Another branch of the PAH family tree is represented by the heterocyclic PAHs and their cations. Nitrogen, in particular, can be exchanged with CH groups to form polycyclic aromatic nitrogen heterocycles (PANHs) (40). As much as half of the nitrogen content of the galactic ISM is unaccounted for (41); thus a substantial quantity of nitrogen may be hidden away in PANHs, which are currently estimated to incorporate more than 1% of the available nitrogen.

Obtaining experimental reaction rates or spectra of PANH cations is challenging as these species—especially those with interior nitrogen atoms, which are the most likely sources of the observed IR emission spectra (40)—are difficult to synthesize.

SIFT: selected ion flow tube

Some neutral PANHs are unstable in the lab because they have unpaired electrons; however, these radicals can survive in the ISM because of the low collision rates. The performance of experimental studies of PANHs and PANH^+ s remains an important challenge to the laboratory astrophysics community.

1.2.6. Reactions forming the first molecules in the universe. Cosmological observations and theory both implicate H_2 as the trigger for the formation of the first stars and galaxies, in short, for the creation of all the complex matter in the universe. In the absence of H_2 , the universe would contain only atomic hydrogen, a small amount of ^3He , and traces of other elements (such as Li and Be) formed in the initial big bang. All of the other elements and isotopes that make up the matter in the universe were created by nucleosynthesis in stellar interiors. And without H_2 , no stars would ever have formed.

H_2 serves as a coolant in star formation through its quadrupole transitions, allowing atomic clouds to condense (42). However, gas-phase reactions forming H_2 are very slow, so most models assume H_2 formation on solid-grain surfaces (43, 44). Although this mechanism is adequate for interstellar clouds containing dust, there was no dust in the beginning. Thus, scientists have invoked associative detachment of H with H^- (45): $\text{H} + \text{H}^- \rightarrow \text{H}_2 + \text{e}^-$.

The rate constant for this crucial reaction has been measured in only one laboratory and has large error bars. Recent work (46) highlights the importance of this reaction rate and explores the consequences of values at either end of the uncertainty range. Clearly, this reaction rate constant must be refined.

2. REVIEW OF LABORATORY STUDIES OF ION-ATOM REACTIONS

2.1. Methods

The development of sophisticated analytical instrumentation has enabled the detailed characterization of the interstellar medium described above. Both ground-based and space-based telescopes with spectroscopic detection capabilities throughout the electromagnetic spectrum have allowed the determination of the chemical and physical properties of the ISM.

Similarly, laboratory studies of relevant chemical reactions have been dependent on the development of analytical techniques with increasingly powerful capabilities. For studies of charged particles, mass spectrometry has provided an exceptionally versatile approach. Studies during the last five decades have utilized ion cyclotron resonance (ICR), flowing afterglow, flowing afterglow–Langmuir probe, Fourier transform mass spectrometry, ion beams, ion traps, ion storage rings, selected ion flow tube (SIFT) instruments, and a low-temperature supersonic flow technique, which has allowed studies of ion chemistry at 10 K (47). Moreover, an array of ionization methods has allowed the generation of both common and exotic ions (48). These approaches have explored a wide variety of processes such as bimolecular ion chemistry ($\text{A}^\pm + \text{B} \rightarrow \text{C}^\pm + \text{D}$), associative detachment ($\text{A}^- + \text{B} \rightarrow \text{AB} + \text{e}^-$), radiative

association ($A^+ + B \rightarrow AB^+ + h\nu$), and dissociative recombination ($AB^+ + e^- \rightarrow A + B$), among others, all of which are important in the ISM. Several reviews and compilations have described the analytical approaches (49, 50) and summarized the available data (51–53).

One of the most challenging areas of laboratory research involves the gas-phase reactions between ions and neutral atoms, as both partners are often highly reactive species. A review of gas-phase ion-atom reactions was published in 1993 by Sablier & Rolando (54). Our paper provides a comprehensive review of laboratory studies done since 1993 of positive ion and negative ion reactions with three atomic species that are important in the ISM: H, N, and O. These studies have been carried out almost exclusively with the SIFT technique; however, several reactions of positive ions with H-atoms have recently been reported utilizing a newly developed multi-electrode ion trap. These instruments, as well as the methods of atom production and measurement, are described below.

2.1.1. The selected ion flow tube. Flow tube techniques for studying gas-phase ion chemistry were first introduced 40 years ago by Ferguson and colleagues (55) at the National Oceanic and Atmospheric Administration laboratories in Boulder, CO. Since that time, the technique has been extended and refined (56, 57) to incorporate temperature (58, 59) and kinetic energy variability (60), a variety of ionic and neutral sources (61), Langmuir probe detection (62), laser interrogation methods (63), triple quadrupole detection (64), and mass selection of the reactant ion (SIFT) (65).

Figure 6 presents a schematic diagram of the SIFT instrument used in our laboratory for the study of ion-atom reactions of interstellar relevance. The apparatus consists of regions for (a) ion production, (b) mass selection and injection of ions, (c) reaction of the ions with neutral reagents, and (d) detection of the ionic reactant and products. Positive and negative ions are generated in a flow of helium by a variety of methods. For example, electron ionization of N_2O generates O^+ , which reacts with CH_4 to form HO^+ . Subsequent addition of acetylene produces $HC\equiv C^+$ by proton abstraction. Carbon chain anions, such as C_7^- , are readily formed by a dc discharge between a graphite rod and the stainless steel flow tube. Molecular cations of PAHs are formed by the Penning ionization reaction of metastable argon (formed in a cold cathode discharge) with the parent PAH. For compounds of low volatility, such as coronene, a resistively heated oven can be utilized to increase the vapor pressure of the neutral in the source flow tube.

The ions are extracted through a nose cone and focused by lenses; the desired ion is mass-selected by the SIFT quadrupole mass filter, refocused by lenses, and injected into the reaction flow tube through a Venturi inlet. The ions are entrained in a flow of helium buffer gas ($P = 0.5$ torr, $F = 200$ atm cm^3 s^{-1}) that provides thermalization of the ions and transport along the flow tube. The neutral reactants (H, N, or O) are added downstream of the ion injection, and the ion-neutral reaction occurs throughout the remainder of the flow tube. Most of the gas mixture is exhausted by a large Roots blower system, and the ions are sampled through a nose cone, mass-analyzed, and detected with an electron multiplier. Rate constants

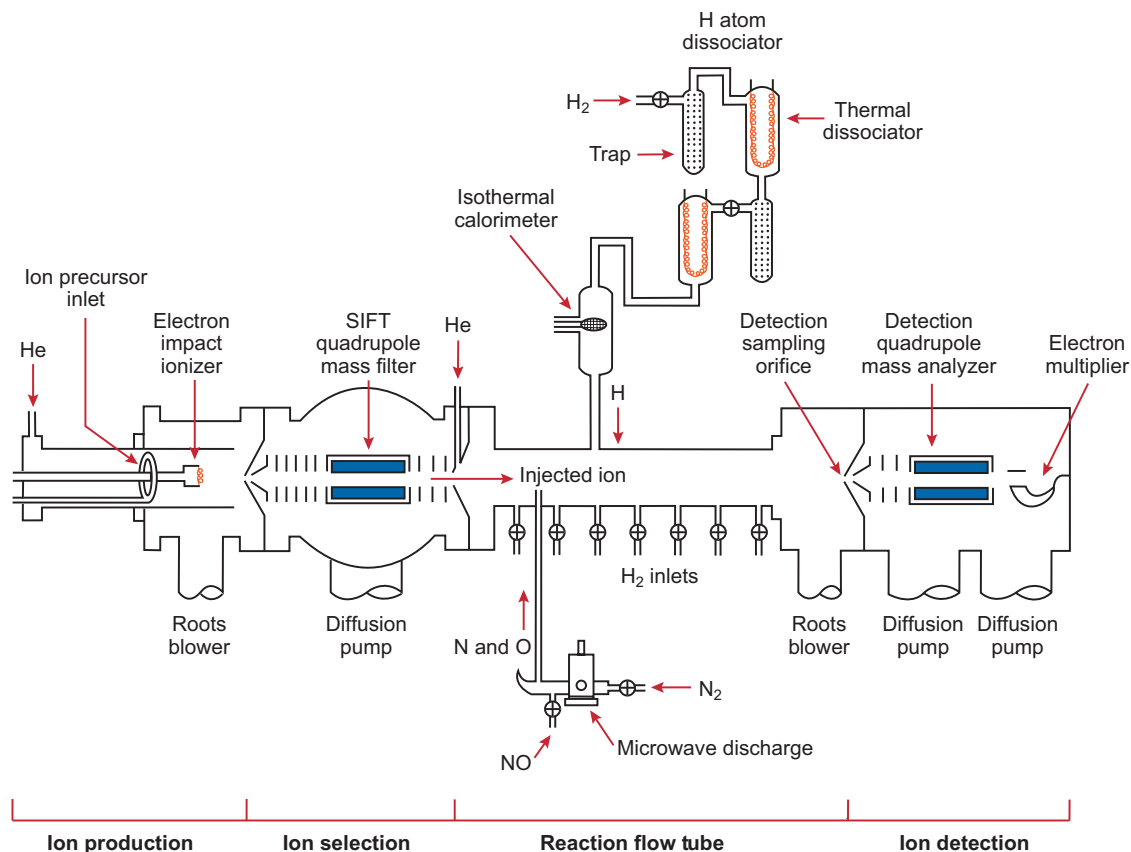


Figure 6

The flowing afterglow–selected ion flow tube (SIFT) instrument. The tandem flow tube instrument allows the production of ions by a variety of ionization techniques, followed by selection of the desired reactant ion with the SIFT quadrupole mass filter, interaction of the ion with atomic or molecular reagents in the reaction flow tube, and detection of reactant and product ions with a quadrupole mass analyzer coupled to an electron multiplier detector.

are determined from the decrease of reactant ion signal with increasing flow rate of the atomic reactant, and other experimental parameters including the pressure and flow of helium, the temperature, and the reaction time. Alternatively, for stable neutral reactants such as molecular hydrogen, the reagent can be introduced into the flow tube through a manifold of inlets, and the reactant ion signal can be monitored as a function of increasing reaction distance. Product distributions are determined by the ratio of the product ions under conditions where mass discrimination is minimized.

One of the most powerful features of flow systems is their capability for studying atomic neutral reactants, including H, N, and O atoms. Hydrogen atoms can be formed by passing molecular hydrogen through a microwave discharge (66).

However, as shown in **Figure 6** our SIFT experiments usually utilize thermal dissociation (67), which produces $\text{H}(^2\text{S})$ atoms in the absence of metastable species. High-purity H_2 flows through a molecular sieve trap immersed in liquid nitrogen, over a heated tungsten filament, and through a second cooled sieve trap. This process efficiently removes trace impurities. The molecular hydrogen is dissociated by passage over a second heated filament, and dissociation ratios of about 30% can be achieved. To introduce the hydrogen atoms into the reaction flow tube, the “isothermal calorimeter” is withdrawn into a side arm. From the exit of the second thermal dissociator to the entrance of the reaction flow tube, the H/H_2 mixture flows through Teflon tubing in order to minimize recombination. To measure the H-atom flow rate, the Teflon tubing is positioned above the isothermal calorimeter, which consists of a platinum wire mesh that efficiently recombines the H-atoms. A self-balancing Kelvin bridge accurately measures the heat released in this process, thereby also measuring the flow rate of the hydrogen atoms. Alternatively, a calibration reaction with known rate constant can be examined to determine the atom flow rate.

$\text{N}(^4\text{S})$ atoms are formed by flowing pure molecular nitrogen through a microwave discharge operating between 10 and 50 W. Phosphoric acid coating of the discharge tube can be utilized to minimize wall recombination, and dissociation ratios of about 2% can be achieved. $\text{O}(^3\text{P})$ atoms are formed by adding NO (5% in helium) immediately downstream of the nitrogen discharge (**Figure 6**) to initiate the quantitative reaction $\text{N} + \text{NO} \rightarrow \text{O} + \text{N}_2$ (68). This method is preferred over direct microwave dissociation of molecular oxygen, which is known to also generate reactive $\text{O}_2(^1\Delta_g)$ metastables. The flow rates of the nitrogen and oxygen atoms are determined by the endpoint of the $\text{N} + \text{NO}$ titration.

2.1.2. The multi-electrode ion trap. Gerlich and colleagues (69, 70) have recently described an innovative instrument for the study of ion-neutral reactions, including atomic neutral reagents, at temperatures as low as 10 K. A schematic diagram of the Atomic Beam 22-Pole Trap apparatus is shown in **Figure 7**. The hydrogen atoms are generated in a radiofrequency (rf) plasma source, which has been optimized to maximize dissociation and minimize recombination. The atoms are cooled by passage through a glass tube at 100 K; they then pass through a copper accommodator with a temperature range of 10–300 K, as determined by a silicon temperature sensor. The effusive beam of H-atoms is skimmed, differentially pumped twice, and focused by two hexapole magnets into the 22-pole trap. The number density of atomic and molecular hydrogen in the reaction region is determined using a calibrated universal detector based on ionization via electron bombardment.

Primary ions are generated in a standard storage ion source, mass-selected with an rf quadrupole, and injected into the trap via an electrostatic quadrupole Bender. The trap is maintained at a temperature between 10–300 K. A variable storage time (milliseconds to seconds) allows the extent of the ion-neutral reaction to be varied and monitored. The ions are then extracted, mass-analyzed, and detected. Due to the high efficiency of trapping, reaction rate constants as low as $10^{-13} \text{ cm}^3 \text{ s}^{-1}$ can be determined by this approach.

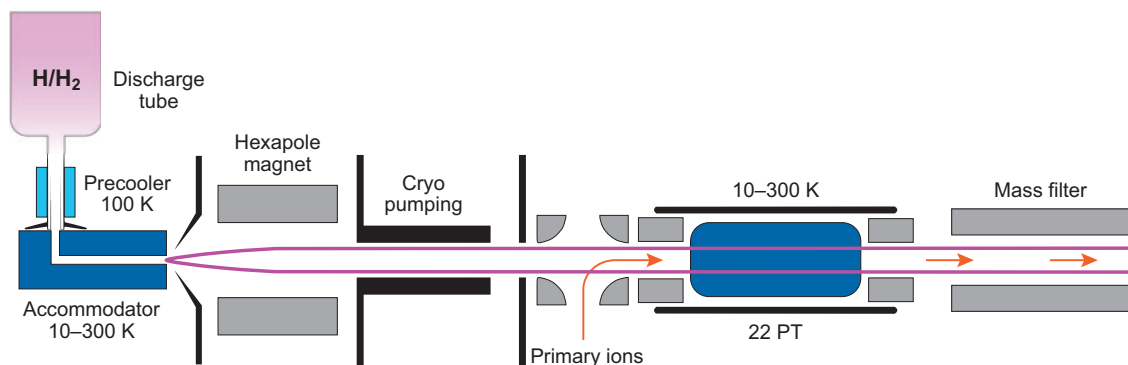


Figure 7

The Atomic Beam 22-Pole Ion Trap. Hydrogen atoms are generated in a radiofrequency plasma source, cooled to temperatures as low as 10 K, and focused by two hexapole magnets into a temperature-variable 22-pole trap (see text for details). Reproduced with permission from Dieter Gerlich.

2.2. Reactions of Positive Ions with Hydrogen, Nitrogen, and Oxygen

Tables 3, 4, and 5 summarize the laboratory studies of the reactions of positive ions with H, N, and O atoms, respectively; these studies have been carried out since the comprehensive review of Sablier & Rolando (54). The reaction products, branching ratios, reaction rate constants, and literature references are tabulated. Ions for which no reactions were observed are also identified.

2.2.1. Positive ions with H-atoms. Although this review focuses on the reactivity of ions with H-atoms, some discussion of reactivity with molecular hydrogen is included as these species inevitably coexist in laboratory experiments. The reactions of aromatic cations with hydrogen atoms are particularly important because PAH cations have been implicated as the carriers of the DIBs. The parent molecular cations of benzene ($C_6H_6^+$), naphthalene ($C_{10}H_8^+$), pyrene ($C_{16}H_{10}^+$), chrysene ($C_{18}H_{12}^+$), and coronene ($C_{24}H_{12}^+$) are radical cations, and they react readily with H-atoms by addition (71–73); only in the case of benzene is there a competing H-atom abstraction channel. Similarly, the radical cations $C_6H_4^+$ and $C_{10}H_6^+$ react efficiently with H-atoms. In contrast, the singlet cations $C_6H_5^+$ and $C_{10}H_7^+$ are essentially unreactive with hydrogen atoms, but react with molecular hydrogen by addition. The observation of this latter process at the low pressures of an ICR indicates that radiative association is occurring, even for these relatively small systems (74); thus these reactions are likely to be important in the diffuse ISM. In analogy to these smaller systems, $C_{16}H_9^+$ might be expected to be a singlet cation and therefore unreactive with H-atoms; however, both theoretical calculations and its high reactivity with hydrogen atoms confirm that $C_{16}H_9^+$ is a triplet cation in its ground state. The reactions of the singlet protonated naphthalene cation ($C_{10}H_9^+$) and protonated pyrene cation ($C_{16}H_{11}^+$) with H-atoms or molecular hydrogen are very slow, suggesting that these protonated species will be terminal ionic species in interstellar environments where

Table 3 Experimental results for the reactions of positive ions^a with H-atoms at 298 (± 5) K, unless otherwise specified

Ionic reactant	Reaction products	Branching ratio	Rate constant (cm ³ s ⁻¹)	Reference
C ₆ H ₆ ⁺ (benzene)	C ₆ H ₇ ⁺	~0.65	2.1 × 10 ⁻¹⁰	76
	C ₆ H ₅ ⁺ + H ₂	~0.35		
C ₁₀ H ₈ ⁺ (naphthalene)	C ₁₀ H ₉ ⁺	1.0	1.9 × 10 ⁻¹⁰	71
C ₁₆ H ₁₀ ⁺ (pyrene)	C ₁₆ H ₁₁ ⁺	1.0	1.4 × 10 ⁻¹⁰	72
C ₁₈ H ₁₂ ⁺ (chrysene)	C ₁₈ H ₁₃ ⁺	1.0	1.8 × 10 ⁻¹⁰	73
C ₂₄ H ₁₂ ⁺ (coronene)	C ₂₄ H ₁₃ ⁺	1.0	1.4 × 10 ⁻¹⁰	73
C ₁₀ H ₆ ⁺	C ₁₀ H ₇ ⁺	1.0	~2 × 10 ⁻¹⁰	71
C ₁₀ H ₇ ⁺	C ₁₀ H ₈ ⁺	1.0	≤ 5 × 10 ⁻¹¹	71
C ₁₀ H ₉ ⁺	C ₁₀ H ₁₀ ⁺	1.0	~4 × 10 ⁻¹²	71
C ₁₆ H ₉ ⁺	C ₁₆ H ₁₀ ⁺	1.0	~1.6 × 10 ⁻¹⁰	72
C ₁₆ H ₁₁ ⁺	C ₁₆ H ₁₂ ⁺	1.0	~3 × 10 ⁻¹²	72
C ₂ H ₃ ⁺	C ₂ H ₂ ⁺ + H ₂	1.0	6.8 × 10 ⁻¹¹	76
H ₂ C ₃ H ₂ ⁺	C ₃ H ₃ ⁺ + H ₂	1.0	1.7 × 10 ⁻¹⁰	76
HC ₃ H ₃ ⁺	C ₃ H ₃ ⁺ + H ₂	1.0	3.0 × 10 ⁻¹⁰	76
C ₃ H ₅ ⁺	C ₃ H ₆ ⁺	1.0	1.6 × 10 ⁻¹⁰	76
C ₃ H ₇ ⁺	C ₃ H ₆ ⁺ + H ₂	1.0	3.2 × 10 ⁻¹¹	76
C ₄ H ⁺	C ₄ H ₂ ⁺	1.0	~5.8 × 10 ⁻¹⁰	76
C ₄ H ₂ ⁺	C ₄ H ₃ ⁺	1.0	2.6 × 10 ⁻¹⁰	76
C ₄ H ₃ ⁺	C ₄ H ₄ ⁺	1.0	~5 × 10 ⁻¹¹	76
C ₄ H ₆ ⁺	C ₂ H ₃ ⁺ + C ₂ H ₄	~0.15	1.9 × 10 ⁻¹⁰	76
	C ₂ H ₅ ⁺ + C ₂ H ₂	~0.65		
	C ₄ H ₅ ⁺ + H ₂	~0.20		
C ₄ H ₈ ⁺	C ₄ H ₇ ⁺ + H ₂	1.0	1.1 × 10 ⁻¹⁰	76
c-C ₆ H ₄ ⁺	C ₆ H ₅ ⁺	1.0	3.3 × 10 ⁻¹¹	76
CO ⁺	H ⁺ + CO	1.0	4.0 × 10 ⁻¹⁰	78
CO ₂ ⁺	HCO ⁺ + O	>0.95	4.7 × 10 ⁻¹⁰	78
	H ⁺ + CO ₂	<0.05		
SO ₂ ⁺	SO ⁺ + OH	1.0	4.2 × 10 ⁻¹⁰	78
CS ₂ ⁺	HCS ⁺ + S	1.0	2.8 × 10 ⁻¹⁰	78
CN ⁺	H ⁺ + CN	1.0	6.4 × 10 ⁻¹⁰	78
C ₂ N ₂ ⁺	HNC ⁺ + CN	0.8	6.2 × 10 ⁻¹⁰	78
	C ₂ H ⁺ + N ₂	0.2		
C ₂ H ₃ ⁺	C ₂ H ₂ ⁺ + H ₂	1.0	6.8 × 10 ⁻¹¹	78
CH ⁺	C ⁺ + H ₂	1.0	1.3 × 10 ⁻⁹ at T _H = T _{ion} = 50 K 8.7 × 10 ⁻¹⁰ at T _H = 100 K, T _{ion} = 80 K	70
CH ₄ ⁺	CH ₃ ⁺ + H ₂	1.0	6.0 × 10 ⁻¹⁰ at T _H = T _{ion} = 50 K 5.1 × 10 ⁻¹⁰ at T _H = 100 K, T _{ion} = 80 K	69, 70
CH ₅ ⁺	CH ₄ ⁺ + H ₂	1.0	9 × 10 ⁻¹² at T _H = 12 K, T _{ion} = 10 K 1.3 × 10 ⁻¹¹ at T _H = T _{ion} = 50 K 2.3 × 10 ⁻¹¹ at T _H = T _{ion} = 100 K	70

^aNo reactions were observed for C₂⁺, C₂H⁺, HC₃H₂⁺, c-C₃H₃⁺, C₄H₅⁺, C₄H₉⁺, ac-C₆H₄⁺, ac-C₆H₅⁺, c-C₆H₅⁺ (76), or NO₂⁺ (78).

Table 4 Experimental results for the reactions of positive ions^a with N-atoms at 298 (± 5) K

Ionic reactant	Reaction products	Branching ratio	Rate constant (cm ³ s ⁻¹)	Reference
C ₆ H ₆ ⁺ (benzene)	C ₅ H ₅ ⁺ + HCN	1.0	1.2 × 10 ⁻¹⁰	71
C ₆ H ₆ ⁺ (benzene)	C ₅ H ₅ ⁺ + HCN	>0.95	1.4 × 10 ⁻¹⁰	79
	C ₃ H ₃ ⁺ + C ₃ H ₃ N	<0.05		
C ₁₀ H ₈ ⁺ (naphthalene)	C ₉ H ₇ ⁺ + HCN	0.3	2.3 × 10 ⁻¹¹	71
	C ₁₀ H ₈ N ⁺	0.7		
C ₁₆ H ₁₀ ⁺ (pyrene)	C ₁₅ H ₉ ⁺ + HCN	<0.05	1.5 × 10 ⁻¹²	72
	C ₁₆ H ₁₀ N ⁺	>0.95		
C ₂₄ H ₁₂ ⁺ (coronene)	None observed		<1 × 10 ⁻¹²	73
C ₁₆ H ₉ ⁺	C ₁₆ H ₉ N ⁺	>0.8	~3 × 10 ⁻¹¹	72
CH ₃ ⁺	HCNH ⁺ + H	0.65	9.4 × 10 ⁻¹¹	79
	HCN ⁺ + H ₂	0.35		
C ₂ H ₂ ⁺	HC ₂ N ⁺ + H	0.60	2.4 × 10 ⁻¹⁰	79
	HCNH ⁺ + C	0.25		
	C ₂ N ⁺ + H ₂	0.10		
	CH ⁺ + HCN	0.05		
C ₂ H ₃ ⁺	HCCN ⁺ + H ₂	>0.90	2.2 × 10 ⁻¹¹	79
	H ₂ CCN ⁺ + H	<0.10		
C ₂ H ₄ ⁺	CH ₂ CNH ⁺ + H	1.0	3.0 × 10 ⁻¹⁰	79
C ₃ ⁺	C ₃ N ⁺	1.0	2.3 × 10 ⁻¹⁰	79
C ₃ H ⁺	C ₃ N ⁺ + H	0.9	2.7 × 10 ⁻¹⁰	79
	HC ₃ N ⁺	0.1		
C ₃ H ₂ ⁺	C ₂ H ₂ ⁺ + CN	0.85	4.4 × 10 ⁻¹¹	79
	HCNH ⁺ + C ₂	0.15		
ac-C ₃ H ₃ ⁺	HC ₃ N ⁺ + H ₂	1.0	5.8 × 10 ⁻¹¹	79
C ₄ H ₂ ⁺	C ₃ H ⁺ + HCN	0.90	1.9 × 10 ⁻¹⁰	79
	C ₄ HN ⁺ + H	0.05		
	HCNH ⁺ + C ₃	0.05		
C ₆ H ₃ ⁺	C ₅ H ⁺ + HCN	1.0	1.9 × 10 ⁻¹⁰	79
c-C ₆ H ₅ ⁺	C ₅ H ₄ ⁺ + HCN	1.0	3.7 × 10 ⁻¹¹	79
CN ⁺	N ₂ ⁺ + C	1.0	6.1 × 10 ⁻¹⁰	80
HCN ⁺	CH ⁺ + N ₂	1.0	2.2 × 10 ⁻¹⁰	80
HC ₃ N ⁺	C ₂ N ⁺ + HCN	0.6	2.4 × 10 ⁻¹⁰	80
	C ₃ H ⁺ + N ₂	0.4		
H ₂ O ⁺	NOH ⁺ + H	0.8	1.4 × 10 ⁻¹⁰	80
	NO ⁺ + H ₂	0.2		
N ₂ ⁺	N ₃ ⁺	1.0	1.4 × 10 ⁻¹¹	80
CO ⁺	NO ⁺ + C	1.0	8.2 × 10 ⁻¹¹	80
O ₂ ⁺	NO ⁺ + O	1.0	1.0 × 10 ⁻¹⁰	80
CO ₂ ⁺	CO ⁺ + NO	1.0	3.4 × 10 ⁻¹⁰	80
H ₃ ⁺	NH ₂ ⁺ + H		4.5 × 10 ⁻¹⁰	94
			<5 × 10 ⁻¹¹	81

^aNo reactions were observed for C₁₀H₇⁺ (71); C₁₆H₁₁⁺ (72); C₂H₅⁺, c-C₃H₃⁺, C₃H₅⁺, C₄H₃⁺, ac-C₆H₅⁺ (79); HCNH⁺, HC₃NH⁺, H₃O⁺, HCO⁺, HCO₂⁺ (80).

Table 5 Experimental results for the reactions of positive ions^a with O-atoms at 298 (± 5) K

Ionic reactant	Reaction products	Branching ratio	Rate constant (cm ³ s ⁻¹)	Reference
C ₆ H ₆ ⁺ (benzene)	C ₅ H ₆ ⁺ + CO	1.0	9.5 × 10 ⁻¹¹	71
C ₆ H ₆ ⁺ (benzene)	C ₅ H ₆ ⁺ + CO	0.9	1.4 × 10 ⁻¹⁰	82
	C ₄ H ₄ O ⁺ + C ₂ H ₂	0.1		
C ₁₀ H ₈ ⁺ (naphthalene)	C ₉ H ₈ ⁺ + CO	0.55	1.0 × 10 ⁻¹⁰	71
	C ₁₀ H ₈ O ⁺	0.45		
C ₁₆ H ₁₀ ⁺ (pyrene)	C ₁₅ H ₁₀ ⁺ + CO	<0.05	9.5 × 10 ⁻¹¹	72
	C ₁₆ H ₁₀ O ⁺	>0.95		
C ₂₄ H ₁₂ ⁺ (coronene)	C ₂₄ H ₁₂ O ⁺	1.0	1.3 × 10 ⁻¹⁰	73
C ₁₆ H ₉ ⁺	C ₁₅ H ₉ ⁺ + CO	~0.5	~2 × 10 ⁻¹⁰	72
	C ₁₆ H ₉ O ⁺	~0.5		
CH ₃ ⁺	HCO ⁺ + H ₂	1.0	4.1 × 10 ⁻¹⁰	82
C ₂ H ₂ ⁺	HCO ⁺ + CH	0.5	2.0 × 10 ⁻¹⁰	82
	HC ₂ O ⁺ + H	0.5		
C ₂ H ₃ ⁺	H ₂ CCO ⁺ + H	0.85	1.0 × 10 ⁻¹⁰	82
	C ₂ H ₃ O ⁺	0.10		
	CH ₃ ⁺ + CO	0.05		
C ₂ H ₄ ⁺	CH ₃ ⁺ + HCO	0.45	2.4 × 10 ⁻¹⁰	82
	HCO ⁺ + CH ₃	0.35		
	HC ₂ O ⁺ + H ₂ + H	0.10		
	CH ₃ CO ⁺ + H	~0.05		
	H ₂ CCO ⁺ + H ₂	~0.05		
ac-C ₃ H ₃ ⁺	C ₃ H ₂ O ⁺ + H	0.30	1.5 × 10 ⁻¹⁰	82
	C ₂ H ₃ ⁺ + CO	0.30		
	C ₂ H ₂ ⁺ + HCO	0.25		
	HC ₃ O ⁺ + H ₂	0.15		
C ₄ H ₂ ⁺	C ₄ HO ⁺ + H	0.50	2.7 × 10 ⁻¹⁰	82
	C ₃ H ₂ ⁺ + CO	0.40		
	C ₃ HO ⁺ + CH	~0.05		
	C ₄ H ₂ O ⁺	~0.05		
c-C ₆ H ₅ ⁺	C ₅ H ₅ ⁺ + CO	0.6	1.0 × 10 ⁻¹⁰	82
	C ₃ H ₃ ⁺ + C ₃ H ₂ O	0.4		
HC ₃ N ⁺	C ₃ NO ⁺ + H	0.50	4.1 × 10 ⁻¹⁰	83
	HC ₂ N ⁺ + CO	0.40		
	HC ₃ NO ⁺	0.10		
N ₂ ⁺	NO ⁺ + N	0.95	1.4 × 10 ⁻¹⁰	83
	O ⁺ + NO	0.05		
H ₃ ⁺	OH ⁺ + H ₂	0.70	1.2 × 10 ⁻⁹	84
	H ₂ O ⁺ + H	0.30		

^aNo reactions were observed for C₁₀H₇⁺ (71); C₁₆H₁₁⁺ (72); C₂H₅⁺, c-C₃H₃⁺, ac-C₃H₃⁺, C₄H₃⁺, ac-C₆H₅⁺ (82); HCNH⁺, H₂C₃N⁺, H₂O⁺, HCO⁺, HCO₂⁺ (83).

^band/or HOC⁺.

they and their derivatives are able to survive. For a comprehensive review of earlier studies of ion-neutral chemistry of PAHs and fullerenes, see Bohme (75).

Based on these and other results, we have modeled (38, 39) the hydrogenation and charge states of PAHs in the ISM for molecules ranging from benzene to those containing 200 carbon atoms. In diffuse clouds, neutral and positively charged species dominate, and the degree of hydrogenation depends strongly on molecular size. Small PAHs (<15–20 carbon atoms) are destroyed in most environments while intermediate-size PAHs (20–30 carbon atoms) are stripped of most peripheral hydrogen atoms. Larger PAHs (>30 carbon atoms) primarily have normal hydrogen coverage (each peripheral carbon atom bears a single hydrogen atom) with competition from the protonated form; these PAHs are good candidates for DIB carriers. Finally, very large PAHs may be fully hydrogenated to give products with two hydrogens on every peripheral carbon atom.

The reactions of a variety of small hydrocarbon cations $C_mH_n^+$ have been reported (76) (**Table 3**). Two types of reaction occur with hydrogen atoms: (1) H-atom transfer to produce $C_mH_{n-1}^+ + H_2$, if this process is exothermic; and (2) association to form $C_mH_{n+1}^+$. With molecular hydrogen as a reactant, highly unsaturated cations undergo primarily hydrogen atom abstraction to form $C_mH_{n+1}^+ + H$; more highly saturated ions are unreactive. McEwan et al. (77) have utilized these data and other experimental and computational results in their model of dense cloud interstellar chemistry. They found that reaction with hydrogen atoms is an important mechanism for increasing the saturation of $C_mH_n^+$ ions with $m > 3$ in dense interstellar clouds, even though the H/H_2 abundance ratio is 10^{-4} . They also concluded that a significant abundance of benzene could be produced in dense clouds through ion-neutral chemistry followed by ion-electron recombination.

The reactions of several oxygen-, sulfur-, and nitrogen-containing cations with hydrogen atoms (78) are also shown in **Table 3**. Reactions proceed by charge transfer, atom transfer, and rearrangement. The rate constants are consistently below the Langevin capture rate, and spin statistics has been identified as the cause in several cases. Notably, the reactant ion CO^+ and three of the product ions (SO^+ , HCO^+ , and HCS^+) have been detected in dense clouds (**Table 1**).

Recent major advances are the development of the 22-pole ion trap instrument and the measurement of ion-hydrogen atom reactions at low temperatures by Gerlich et al. (69, 70). These researchers have reported the reactions of CH^+ , CH_4^+ , and CH_5^+ with hydrogen atoms, which proceed by hydrogen abstraction to form molecular hydrogen and C^+ , CH_3^+ , and CH_4^+ , respectively. The reactions of both CH^+ and CH_4^+ are rapid at low temperatures and decrease slightly with increasing temperature. In contrast, the reaction of CH_5^+ is extremely slow at 10 K and increases slightly as the temperature increases. A more complete understanding of these experimental results remains a significant challenge for theorists.

2.2.2. Positive ions with N-atoms. Although molecular nitrogen is relatively unreactive with most ions due to its strong triple bond and high ionization energy, nitrogen atoms exhibit moderate reactivity and rich chemistry. Reaction of N-atom with $C_6H_6^+$ proceeds by abstraction of CH to generate $C_5H_5^+$ and the interstellar

neutral hydrogen cyanide (HCN). This pathway rapidly decreases in importance as the aromatic cation increases in size, and simple addition dominates (71–73). For hydrocarbon cations (79) and other small positive ions (80), various product channels are formed in which nitrogen is incorporated into the ionic or neutral product. These reactions provide potential mechanisms for generating the nitriles and other nitrogen-containing species detected in the ISM. The rate constant for the important reaction of $\text{H}_3^+ + \text{N}$ has been recently refined to be less than $5 \times 10^{-11} \text{ cm}^3 \text{ s}^{-1}$ (81).

2.2.3. Positive ions with O-atoms. Atomic oxygen is remarkably reactive with small aromatic and PAH cations. For C_6H_6^+ the major pathway is extrusion of a carbon atom from the ring to form C_5H_6^+ and CO. Although the rate constant remains moderately large, simple addition dominates the reactivity for the pyrene and coronene cations (71–73). The reactions of hydrocarbon cations with O-atoms generally proceed at a substantial fraction of the collision rate; the processes occur by multiple channels and show C–O bond formation in the ionic or neutral product (82). The rate constants and product branching ratios for the important reaction of O-atoms with N_2^+ (83) and H_3^+ (84) have been remeasured using the SIFT technique.

2.3. Reactions of Negative Ions with Hydrogen, Nitrogen, and Oxygen

Tables 6, 7, and 8 summarize the laboratory studies of the reactions of negative ions with H, N, and O atoms, respectively, which have been carried out since 1993. The reaction products, branching ratios, reaction rate constants, and literature references are tabulated. Ions for which no reactions were observed are listed in the footnotes.

2.3.1. Negative ions with H-atoms. Our studies (85) of the reactions of carbon chain anions and hydrogenated carbon chain anions were prompted by the proposal (86) that C_7^- might form some of the DIBs, and by the fact that unsaturated hydrocarbon species have been detected in the ISM. The recent discovery of C_4H^- , C_6H^- , and C_8H^- in the ISM confirms the relevance of these anions. We found that C_n^- anions react rapidly with H-atoms by associative detachment, with larger ions ($n \geq 7$) also reacting by association. The hydrogenated carbon chain anions react exclusively by rapid associative detachment. None of these ions reacts with molecular hydrogen. Similarly, Viggiano and colleagues (87) have found that the small fluorinated hydrocarbon anions CF_3^- , C_2F_5^- , and C_3F_3^- react by associative detachment with H and are unreactive with H_2 . This research group has also explored the reactivity of fluorinated anions containing sulfur (88) and chlorinated anions containing phosphorus (89) with H-atoms as a function of temperature. Halogen atom abstraction dominates, and the reactions show only small changes in reactivity between 300 and 500 K.

2.3.2. Negative ions with N-atoms. The carbon chain anions and hydrogenated carbon chain anions are unreactive with N_2 but react at moderate rates with N-atoms (90). Associative detachment occurs for all ions, and several atom transfer and

Table 6 Experimental results for the reactions of negative ions^a with H-atoms at 298 (± 5) K, unless otherwise specified

Ionic reactant	Reaction products	Branching ratio	Rate constant (cm ³ s ⁻¹)	Reference
C ₂ ⁻	C ₂ H + e ⁻	1.0	7.7 × 10 ⁻¹⁰	85
C ₄ ⁻	C ₄ H + e ⁻	1.0	6.2 × 10 ⁻¹⁰	85
C ₅ ⁻	C ₅ H + e ⁻	1.0	6.2 × 10 ⁻¹⁰	85
C ₆ ⁻	C ₆ H + e ⁻	1.0	6.1 × 10 ⁻¹⁰	85
C ₇ ⁻	C ₇ H + e ⁻	0.41	6.9 × 10 ⁻¹⁰	85
	C ₇ H ⁻	0.59		
C ₈ ⁻	C ₈ H + e ⁻	0.33	7.3 × 10 ⁻¹⁰	85
	C ₈ H ⁻	0.67		
C ₉ ⁻	C ₉ H + e ⁻	0.17	7.2 × 10 ⁻¹⁰	85
	C ₉ H ⁻	0.83		
C ₁₀ ⁻	C ₁₀ H + e ⁻	0.24	7.5 × 10 ⁻¹⁰	85
	C ₁₀ H ⁻	0.76		
HC ₂ ⁻	C ₂ H ₂ + e ⁻	1.0	1.6 × 10 ⁻⁹	85
HC ₄ ⁻	C ₄ H ₂ + e ⁻	1.0	8.3 × 10 ⁻¹⁰	85
HC ₆ ⁻	C ₆ H ₂ + e ⁻	1.0	5.0 × 10 ⁻¹⁰	85
HC ₇ ⁻	C ₇ H ₂ + e ⁻	1.0	7.4 × 10 ⁻¹⁰	85
CF ₃ ⁻	Product + e ⁻	1.0	5.3 × 10 ⁻¹⁰	87
C ₂ F ₅ ⁻	Product + e ⁻	1.0	6.0 × 10 ⁻¹⁰	87
C ₃ F ₃ ⁻	Product + e ⁻	1.0	9.0 × 10 ⁻¹⁰	87
F ⁻	HF + e ⁻	1.0	1.4 × 10 ⁻⁹ at 500 K ^b	88
SF ₆ ⁻	SF ₅ ⁻ + HF	1.0	3.1 × 10 ⁻¹⁰ at 298 K	88
			2.5 × 10 ⁻¹⁰ at 500 K	
SOF ₄ ⁻	SOF ₃ ⁻ + HF	1.0	1.8 × 10 ⁻¹⁰ at 298 K	88
			1.2 × 10 ⁻¹⁰ at 500 K	
SO ₂ ⁻	<i>cis</i> -HOSO + e ⁻	1.0	2.3 × 10 ⁻¹⁰ at 298 K	88
			2.6 × 10 ⁻¹⁰ at 500 K	
SO ₂ F ₂ ⁻	SO ₂ F ⁻ + HF	1.0	3.2 × 10 ⁻¹⁰ at 298 K	88
			2.6 × 10 ⁻¹⁰ at 500 K	
PO ₂ Cl ⁻	PO ₂ ⁻ + HCl	1.0	3.6 × 10 ⁻¹⁰ at 300 K	89
			3.7 × 10 ⁻¹⁰ at 500 K	
POCl ₂ ⁻	POCl ⁻ + HCl	0.94	1.6 × 10 ⁻¹⁰ at 300 K	89
	Cl ⁻ + HPOCl	0.06	1.6 × 10 ⁻¹⁰ at 500 K	
POCl ₃ ⁻	POCl ₂ ⁻ + HCl	1.0	3.8 × 10 ⁻¹⁰ at 300 K	89
			3.7 × 10 ⁻¹⁰ at 500 K	

^aNo reactions were observed for SF₅⁻, SOF₃⁻, SO₂F⁻ (88); PO₂Cl₂⁻ (89).

^bMeasured relative to the rate constant (1.6 × 10⁻⁹) at 298 K (95).

fragmentation channels appear, with formation of C-N bonds. Several of these nitrile species, including CN, C₃N, C₅N, HC₂N, and HC₄N, have been detected in the ISM. Unfortunately, it was not possible to determine the branching ratios for these processes due to the occurrence of rapid secondary reactions.

Recent measurements (91) have found that the rate constant for O₂⁻ + N is a factor of two slower than previously determined, and that a second product channel (O⁻ + NO, 35%) occurs in addition to the associative detachment reported earlier.

Table 7 Experimental results for the reactions of negative ions^a with N-atoms at 298 (± 5) K

Ionic reactant	Reaction products	Branching ratio	Rate constant (cm ³ s ⁻¹)	Reference
C ₂ ⁻	CN ⁻ + C C ₂ N + e ⁻		2.3 × 10 ⁻¹⁰	90
C ₄ ⁻	CN ⁻ + C ₃ C ₃ ⁻ + CN C ₄ N + e ⁻		2.0 × 10 ⁻¹⁰	90
C ₅ ⁻	CN ⁻ + C ₄ C ₄ ⁻ + CN C ₃ N ⁻ + C ₂ C ₅ N + e ⁻		2.7 × 10 ⁻¹⁰	90
C ₆ ⁻	CN ⁻ + C ₅ C ₅ ⁻ + CN C ₃ N ⁻ + C ₃ C ₆ N + e ⁻		1.5 × 10 ⁻¹⁰	90
C ₇ ⁻	CN ⁻ + C ₆ C ₆ ⁻ + CN C ₃ N ⁻ + C ₄ C ₅ N ⁻ + C ₂ C ₇ N + e ⁻		2.2 × 10 ⁻¹⁰	90
HC ₂ ⁻	HCCN + e ⁻	1.0	5 × 10 ⁻¹¹	90
HC ₄ ⁻	CN ⁻ + HC ₃ CN + HC ₃ ⁻ HC ₄ N + e ⁻		~6 × 10 ⁻¹²	90
HC ₆ ⁻	CN ⁻ + HC ₅ C ₃ N ⁻ + HC ₃ HC ₆ N + e ⁻		~1 × 10 ⁻¹¹	90
O ₂ ⁻	NO ₂ + e ⁻ O ⁻ + NO	0.65 0.35	2.3 × 10 ⁻¹⁰	91
SO ₂ ⁻	SO ⁻ + NO S ⁻ + NO ₂	>0.90 <0.10	1.8 × 10 ⁻¹⁰	88
PO ₂ Cl ⁻	PO ₂ ⁻ + NCl PO ₂ N ⁻ + Cl	0.34 0.66	8.0 × 10 ⁻¹¹	92

^aNo reactions were observed for SF₅⁻, SF₆⁻, SO₂F⁻, SO₂F₂⁻, SOF₃⁻, SOF₄⁻ (88); POCl₃⁻, POCl₂⁻ (92).

Rate constants and product branching ratios were recently determined for the reactions of SO₂⁻ (88) and PO₂Cl⁻ (92) with N-atoms; various other ions (**Table 7**) were found to be unreactive.

2.3.3. Negative ions with O-atoms. Oxygen atoms react rapidly with carbon chain anions and hydrogenated carbon chain anions by carbon atom abstraction to generate carbon monoxide; associative detachment also occurs (90). Moreover, for the hydrogenated anions, oxygen/hydrogen exchange is observed. The rate constants for several of these reactions exceed the Langevin collision rate; a new approach that includes the polarizability of the anion has been developed and provides good agreement with experiments (93).

Table 8 Experimental results for the reactions of negative ions with O-atoms at 298 (± 5) K

Ionic reactant	Reaction products	Branching ratio	Rate constant ($\text{cm}^3 \text{s}^{-1}$)	Reference
C_2^-	$\text{C}^- + \text{CO}$ $\text{C}_2\text{O} + \text{e}^-$		5.8×10^{-10}	90
C_4^-	$\text{C}_3^- + \text{CO}$ $\text{C}_4\text{O} + \text{e}^-$		5.6×10^{-10}	90
C_5^-	$\text{C}_4^- + \text{CO}$ C_5O^- $\text{C}_5\text{O} + \text{e}^-$		6.4×10^{-10}	90
C_6^-	$\text{C}_5^- + \text{CO}$ $\text{C}_6\text{O} + \text{e}^-$		4.7×10^{-10}	90
C_7^-	$\text{C}_6^- + \text{CO}$ $\text{C}_7\text{O} + \text{e}^-$		5.3×10^{-10}	90
HC_2^-	$\text{HC}^- + \text{CO}$ $\text{H} + \text{C}_2\text{O}^-$ $\text{HC}_2\text{O} + \text{e}^-$		6.2×10^{-10}	90
HC_4^-	$\text{HC}_3^- + \text{CO}$ $\text{H} + \text{C}_4\text{O}^-$ $\text{HC}_4\text{O} + \text{e}^-$		5.3×10^{-10}	90
HC_6^-	$\text{HC}_5^- + \text{CO}$ $\text{H} + \text{C}_6\text{O}^-$ $\text{HC}_6\text{O} + \text{e}^-$		5.4×10^{-10}	90
O_2^-	$\text{O}_3 + \text{e}^-$ $\text{O}^- + \text{O}_2$	<0.55 >0.45	3.9×10^{-10}	91
SF_5^-	$\text{F}^- + \text{SOF}_4$	1.0	5.4×10^{-11}	88
SF_6^-	$\text{O}^- + \text{SF}_6$	1.0	1.1×10^{-10}	88
SO_2F^-	$\text{F}^- + \text{SO}_3$ $\text{SO}_3^- + \text{F}$	0.60 0.40	1.5×10^{-10}	88
SO_2F_2^-	$\text{SO}_3\text{F}^- + \text{F}$	1.0	9.1×10^{-11}	88
SO_2^-	$\text{O}^- + \text{SO}_2$	1.0	4.0×10^{-10}	88
SOF_3^-	$\text{SO}_2\text{F}_2^- + \text{F}$	1.0	7.7×10^{-11}	88
SOF_4^-	$\text{F}^- + (\text{SO}_2\text{F}_2 + \text{F})$	1.0	7.9×10^{-11}	88
POCl_3^-	$\text{POCl}_2^- + \text{ClO}$	1.0	3.9×10^{-10}	92
POCl_2^-	$\text{PO}_2\text{Cl}^- + \text{Cl}$ $\text{Cl}^- + \text{PO}_2\text{Cl}$ $\text{PO}_2^- + \text{Cl}_2$ $\text{Cl}_2^- + \text{PO}_2$	≥ 0.84 ≤ 0.09 ≤ 0.04 ≤ 0.03	3.7×10^{-10}	92
PO_2Cl^-	$\text{PO}_2^- + \text{ClO}$ $\text{PO}_3^- + \text{Cl}$	0.34 0.66	2.6×10^{-10}	92

The newly determined rate constant (91) for reaction of O_2^- with oxygen atom is slightly larger than the previously reported value. Reactions of fluorinated sulfur anions show charge transfer and F-atom or F^- exchange in the reactant ion (88). Reactions of PO_xCl_y^- are rapid and proceed primarily by loss of chlorine from the reactant ion (92).

SUMMARY POINTS

1. The ISM is extremely heterogeneous with a broad range of temperatures, densities, and extinction parameters.
2. Spectroscopic observations throughout the electromagnetic spectrum have detected more than 140 molecular species in the ISM, despite the relatively hostile conditions.
3. Chemical modeling of interstellar clouds relies on accurate laboratory data, including rates and products of ion-neutral reactions.
4. Studies of ion-atom reactions pose unique experimental challenges. Two innovative techniques, the SIFT and the multi-electrode ion trap, have proven to be powerful approaches for these studies.
5. The past fifteen years have seen active research in experimental studies of both positive and negative ions reacting with hydrogen, nitrogen, and oxygen atoms; many of these systems are relevant to interstellar chemistry.

FUTURE ISSUES

1. Laboratory studies of ion-atom reactions at extremely low temperatures with newly developed instrumentation will provide unprecedented data.
2. The detection of negative ions in the ISM highlights the need for a comprehensive understanding of negative ion chemistry.
3. Experiments with other atoms, especially carbon, and with molecular radicals detected in interstellar clouds pose challenges for future studies of ion reactions.
4. Large PAHs, as well as PAHs containing nitrogen and oxygen, are possible carriers of the diffuse interstellar bands; experimental studies of their ion chemistry are essential.
5. Additional studies of other gas-phase reactions, including radiative association and dissociative recombination, as well as full characterization of their products, are critical for developing accurate chemical models of interstellar clouds. Synthetic routes to biological models remain an intriguing challenge.
6. The future of astrochemistry is bright: The synergy of astronomical observations and laboratory studies will continue to advance our understanding of both the ISM and its fundamental chemical processes.

DISCLOSURE STATEMENT

The authors are not aware of any biases that might be perceived as affecting the objectivity of this review.

ACKNOWLEDGMENTS

We gratefully acknowledge support of our research by the National Aeronautics and Space Administration. We thank Dieter Gerlich for generously supplying **Figure 7** as well as unpublished results, and we acknowledge many colleagues for responding to our request for information: Nigel Adams, Peter Barnes, Edwin Bergin, Stephen Blanksby, Diethard Bohme, Andre Canosa, Eric Herbst, Jan M. Hollis, Eva Kovacevic, Harvey Liszt, Murray McEwan, Tom Millar, Holger Mueller, Mark Smith, Albert Viggiano, Valentine Wakelam, Adam Walters, Mark Wolfire, Daniel Wolf-Savin, Paul Woods, and David Woon. We thank Joshua Destree, Kimberly Johnson, Oscar Martinez, and Teresa Ross for assistance with figures and tables.

LITERATURE CITED

- Herbst E. 2001. The chemistry of interstellar space. *Chem. Soc. Rev.* 30:168–76
- Smith D. 1992. The ion chemistry of interstellar clouds. *Chem. Rev.* 92:1473–85
- Dunham T. 1937. Interstellar neutral potassium and neutral calcium. *Pub. Astron. Soc. Pacific* 49:26–28
- McKellar A. 1940. Evidence for the molecular origin of some hitherto unidentified interstellar lines. *Pub. Astron. Soc. Pacific* 52:187–92
- Adams WS. 1941. Some results with the coudé spectrograph of the Mount Wilson Observatory. *Astrophys. J.* 93:11
- Douglas AE, Herzberg G. 1941. CH^+ in interstellar space and in the laboratory [note]. *Astrophys. J.* 94:381
- Bates DR, Spitzer L. 1951. The density of molecules in interstellar space. *Astrophys. J.* 113:441–63
- Solomon PM, Klemperer W. 1972. The formation of diatomic molecules in interstellar clouds. *Astrophys. J.* 178:389–422
- Watson WD. 1973. Interstellar molecular reactions. *Rev. Modern Phys.* 48:13–52
- Dalgarno A. 2000. In *Astrochemistry: Historical Perspective and Future Challenges*. Presented at IAU Symp. 197, p. 1, Aug. 23–27, 1999, Sogwipo, Cheju, Korea
- Weinreb S, Barrett AH, Meeks ML, Henry JC. 1963. Radiospectroscopic observations of OH in interstellar space. *Nature* 200:829–31
- Rydbeck OEH, Hjalmarson A. 1985. Radio observations of interstellar molecules, of their behavior, and of their physics. In *Molecular Astrophysics: State of the Art and Future Directions*, pp. 45–174. Bad Windsheim, Germany: Dordrecht: Reidel
- Thorwirth S. 2007. et seq. The Cologne Database for Molecular Spectroscopy. <http://www.ph1.uni-koeln.de/vorhersagen/>
- Kuan Y-J, Charnley SB, Huang H-C, Tseng W-L, Kisiel Z. 2003. Interstellar glycine. *Astrophys. J.* 593:848–67
- Snyder LE, Lovas FJ, Hollis JM, Friedel DN, Jewell PR, et al. 2005. A rigorous attempt to verify interstellar glycine. *Astrophys. J.* 619:914–30
- Cernicharo J, Guélin M, Agúndez M, Kawaguchi K, McCarthy M, Thaddeus P. 2007. Astronomical detection of C_4H^- , the second interstellar anion. *Astron. Astrophys. J.* 467:L37–L40

17. McCarthy MC, Gottlieb CA, Gupta H, Thaddeus P. 2006. Laboratory and astronomical identification of the negative molecular ion C_6H^- . *Astrophys. J. Lett.* 652:L141–44
18. Remijan AJ, Hollis JM, Lovas FJ, Cordiner MA, Millar TJ. 2007. Detection of C_8H^- and comparison with C_8H toward IRC +10 216. *Astrophys. J. Lett.* 664:L47–L50
19. Allamandola LJ, Tielens AGGM, Barker JR. 1989. Interstellar polycyclic aromatic hydrocarbons: the infrared emission bands, the excitation/emission mechanism, and the astrophysical implications. *Astrophys. J. Supp.* 71:733–75
20. Puget JL, Léger A. 1989. A new component of the interstellar matter: small grains and large aromatic molecules. *Ann. Rev. Astron. Astrophys.* 27:161–98
21. Léger A, D'Hendecourt L, Boccarda N, eds. 1987. *Polycyclic Aromatic Hydrocarbons and Astrophysics*, vol. 191. Dordrecht, Neth.: Reidel
22. Gautier TN, Fink U, Larson HP, Treffers RR. 1976. Detection of quadrupole emission in the Orion Nebula. *Astrophys. J. Lett.* 207:L129–L33
23. Shull JM, Beckwith S. 1982. Interstellar molecular hydrogen. *Ann. Rev. Astron. Astrophys.* 20:163–90
24. Lacy JH, Knacke R, Geballe TR, Tokunaga AT. 1994. Detection of absorption by H_2 in molecular clouds: a direct measurement of the $H_2:CO$ ratio. *Astrophys. J. Lett.* 428:L69–L72
25. Black JH, Willner SP. 1984. Interstellar absorption lines in the infrared spectrum of NGC 2024 IRS 2. *Astrophys. J.* 279:673–78
26. Snow TP, McCall BJ. 2006. Diffuse atomic and molecular clouds. *Ann. Rev. Astron. Astrophys.* 44:367–414
27. Markwick-Kemper AJ. 2005. The most important reactions in gas-phase astrochemical models. In *Astrochemistry: Recent Successes and Current Challenges*. Presented at IAU Symp. 231, Aug. 29–Sept. 2, 2004, Pacific Grove, CA
28. Wakelam V, Herbst E, Selsis F. 2006. The effect of uncertainties on chemical models of dark clouds. *Astron. Astrophys.* 451:551–62
29. Woodall J, Agúndez M, Markwick-Kemper AJ, Millar TJ. 2007. The UMIST database for astrochemistry 2007. *Astron. Astrophys. J.* 466:1197–204
30. Herbst E. 2007. www.physics.ohio-state.edu/~eric/
31. Millar TJ, Walsh C, Cordiner MA, Chuimín RN, Herbst E. 2007. Hydrocarbon anions in interstellar clouds and circumstellar envelopes. *Astrophys. J. Lett.* 662:L87–L90
32. Le Petit F, Nehmé C, Le Bourlot J, Roueff E. 2006. A model for atomic and molecular interstellar gas: The Meudon PDR Code. *Astrophys. J. Suppl.* 164:506–29
33. Stepanovic M, Betts NB, Eichelberger BR, Snow TP, Bierbaum VM. 2008. Gas phase reactions of organic anions with atoms. Manuscript in preparation
34. Blagojevic V, Petrie S, Bohme DK. 2003. Gas-phase syntheses for interstellar carboxylic and amino acids. *Mon. Not. R. Astron. Soc.* 339:L7–L11
35. Heger ML. 1922. Further study of the sodium lines in class B stars; The spectra of certain class B stars in the regions 5630Å–6680Å and 3280Å–3380Å; Note on the spectrum of γ Cassiopeiae between 5860Å and 6600Å. *Lick Observatory Bull.* No. 337:141–48

36. Herbig GH. 1995. The diffuse interstellar bands. *Ann. Rev. Astron. Astrophys.* 33:19–73
37. Snow TP. 2001. The unidentified diffuse interstellar bands as evidence for large organic molecules in the interstellar medium. *Spectrochim. Acta, Part A* 75:615–26
38. Le Page V, Snow TP, Bierbaum VM. 2001. Hydrogenation and charge states of PAHs in diffuse clouds. I. Development of a model. *Astrophys. J. Suppl.* 132:233–51
39. Le Page V, Snow TP, Bierbaum VM. 2003. Hydrogenation and charge states of PAHs in diffuse clouds. II. Results. *Astrophys. J.* 584:316–30
40. Hudgins DM, C. W. Bauschlicher J, Allamandola LJ. 2005. Variations in the peak position of the 6.2 μm interstellar emission feature: a tracer of N in the interstellar polycyclic aromatic hydrocarbon population. *Astrophys. J.* 632:316–32
41. Jensen AG, Snow TP. 2007. Is there enhanced depletion of gas-phase nitrogen in moderately reddened lines of sight? *Astrophys. J.* 654:955–70
42. Lepp S, Stancil PC, Dalgarno A. 2002. Atomic and molecular processes in the early universe. *J. Phys. B: At. Mol. Opt. Phys.* 35:R57–R80
43. Gould RJ, Salpeter EE. 1963. The interstellar abundance of the hydrogen molecule. I. Basic processes. *Astrophys. J.* 138:393–407
44. Hollenbach D, Salpeter EE. 1971. Surface recombination of hydrogen molecules. *Astrophys. J.* 163:155–64
45. McDowell MRC. 1961. On the formation of H_2 in H I regions. *Observatory* 81:240–43
46. Glover SC, Savin DW, Jappsen A-K. 2005. Cosmological implications of the uncertainty in H^- destruction rate coefficients. *Astrophys. J.* 640:553–68
47. Smith IWM, Rowe BR. 2000. Reaction kinetics at very low temperatures: laboratory studies and interstellar chemistry. *Acc. Chem. Res.* 33:261–68
48. Vestal ML. 2001. Methods of ion generation. *Chem. Rev.* 101:361–75
49. McLuckey SA, Wells JM. 2001. Mass analysis at the advent of the 21st century. *Chem. Rev.* 101:571–606
50. Petrie S, Bohme DK. 2003. Mass spectrometric approaches to interstellar chemistry. *Top. Curr. Chem.* 225:37–75
51. Ikezoe Y, Matsuoaka S, Takebe M, Viggiano A. 1987. *Gas Phase Ion-Molecule Reaction Rate Constants Through 1986*. Tokyo: Maruzen
52. Anicich VG. 1993. A survey of bimolecular ion-molecule reactions for use in modeling the chemistry of planetary atmospheres, cometary comae, and interstellar clouds: 1993 supplement. *Astrophys. J. Suppl.* 84:215–315
53. Anicich VG. 1993. Evaluated bimolecular ion-molecule gas phase kinetics of positive ions for use in modeling planetary atmospheres, cometary comae, and interstellar clouds. *J. Phys. Chem. Ref. Data* 22:1469–569
54. Sablier M, Rolando C. 1993. Gas-phase ion-atom reactions. *Mass Spectrom. Rev.* 12:285–312
55. Ferguson EE, Fehsenfeld FC, Schmeltekopf AL. 1969. Flowing afterglow measurements of ion-neutral reactions. *Adv. At. Mol. Phys.* 5:1–56
56. Graul ST, Squires RR. 1988. Advances in flow reactor techniques for the study of gas-phase ion chemistry. *Mass Spectrom. Rev.* 7:263–358

57. Bierbaum VM. 2003. Instrumentation: flow tubes. In *The Encyclopedia of Mass Spectrometry*, ed. PB Armentrout, pp. 98–109. Amsterdam, Neth.: Elsevier
58. Dunkin DB, Fehsenfeld FC, Schmeltekopf AL, Ferguson EE. 1968. Ion-molecule reaction studies from 300 to 600 K in a temperature-controlled flowing afterglow system. *J. Chem. Phys.* 49:1365–71
59. Hierl PM, Friedman JF, Miller TM, Dotan I, Mendendez-Barreto M, et al. 1996. Flowing afterglow apparatus for the study of ion-molecule reactions at high temperatures. *Rev. Sci. Instrum.* 67:2142–48
60. McFarland M, Albritton DL, Fehsenfeld FC, Ferguson EE, Schmeltekopf AL. 1973. Flow-drift technique for ion mobility and ion-molecule reaction rate constant measurements. I. Apparatus and mobility measurements. *J. Chem. Phys.* 59:6610–19
61. Poutsma JC, Seburg RA, Chyall LJ, Sunderlin LS, Hill BT, et al. 1997. Combining electrospray ionization and the flowing afterglow method. *Rapid Commun. Mass Spectrom.* 11:489–93
62. Smith D, Adams NG. 1984. Studies of plasma reaction processes using a flowing-afterglow/Langmuir probe apparatus. In *Swarms of Ions and Electrons in Gases*, ed. W Lindinger, TD Märk, F Howorka, pp. 194–217. Vienna, Austria: Springer
63. Bierbaum VM, Ellison GB, Leone SR. 1984. Flowing afterglow studies of ion reaction dynamics. In *Gas Phase Ion Chemistry*, ed. MT Bowers, pp. 1–39. New York: Academic
64. Squires RR, Lane KR, Lee RE, Wright LG, Wood KV, Cooks RG. 1985. A tandem flowing afterglow-triple quadrupole instrument. *Int. J. Mass Spectrom. Ion Proc.* 64:185–91
65. Adams NG, Smith D. 1976. The selected ion flow tube: a technique for studying ion-neutral reactions. *Int. J. Mass Spectrom. Ion Phys.* 21:349–59
66. Setser DW, Kolts JH. 1979. Electronically excited long-lived states of atoms and diatomic molecules in flow systems. In *Reactive Intermediates in the Gas Phase*, ed. DW Setser, pp. 152. New York: Academic
67. Trainor DW, Ham DO, Kaufman F. 1973. Gas phase recombination of hydrogen and deuterium atoms. *J. Chem. Phys.* 58:4599–609
68. Goldan PD, Schmeltekopf AL, Fehsenfeld FC, Schiff HL, Ferguson EE. 1966. Thermal energy ion-neutral reaction rates. II. Some reactions of ionospheric interest. *J. Chem. Phys.* 44:4095–103
69. Gerlich D, Smith M. 2006. Laboratory astrochemistry: studying molecules under inter- and circumstellar conditions. *Phys. Scr.* 73:C25–C31
70. Luca A, Borodi G, Gerlich D. 2006. Interactions of ions with hydrogen atoms. In *Progress Rep. XXIV ICPEAC 2005*, ed. FD Colavecchia, PD Fainstein, J Fiol, MAP Lima, JE Miraglia, et al., p. 20. Rosario, Argent.
71. Le Page V, Keheyan Y, Snow TP, Bierbaum VM. 1999. Reactions of cations derived from naphthalene with molecules and atoms of interstellar interest. *J. Am. Chem. Soc.* 121:9435–46
72. Le Page V, Keheyan Y, Snow TP, Bierbaum VM. 1999. Gas phase chemistry of pyrene and related cations with molecules and atoms of interstellar interest. *Int. J. Mass Spectrom.* 185/186/187:949–59

73. Betts NB, Stepanovic M, Snow TP, Bierbaum VM. 2006. Gas-phase study of coronene cation reactivity of interstellar relevance. *Ap. J.* 651:L129–L131
74. Snow TP, Le Page V, Keheyan Y, Bierbaum VM. 1998. The interstellar chemistry of PAH cations. *Nature* 391:259–60
75. Bohme DK. 1992. PAH and fullerene ions and ion/molecule reactions in interstellar and circumstellar chemistry. *Chem. Rev.* 92:1487–508
76. Scott GBI, Fairley DA, Freeman CG, McEwan MJ, Adams NG, Babcock LM. 1997. $C_mH_n^+$ reactions with H and H_2 : an experimental study. *J. Phys. Chem. A* 101:4973–78
77. McEwan MJ, Scott GBI, Adams NG, Babcock LM, Terzieva R, Herbst E. 1999. New H and H_2 reactions with small hydrocarbon ions and their roles in benzene synthesis in dense interstellar clouds. *Ap. J.* 513:287–93
78. Scott GB, Fairley DA, Freeman CG, McEwan MJ, Spanel P, Smith D. 1997. Gas phase reactions of some positive ions with atomic and molecular hydrogen at 300 K. *J. Chem. Phys.* 106:3982–87
79. Scott GBI, Fairley DA, Freeman CG, McEwan MJ, Anicich VG. 1999. $C_mH_n^+$ reactions with atomic and molecular nitrogen: an experimental study. *J. Phys. Chem. A* 103:1073–77
80. Scott GBI, Fairley DA, Freeman CG, McEwan MJ, Anicich VG. 1998. Gas-phase reactions of some positive ions with atomic and molecular nitrogen. *J. Chem. Phys.* 109:9010–14
81. Milligan DB, Fairley DA, Freeman CG, McEwan MJ. 2000. A flowing afterglow selected ion flow tube (FA/SIFT) comparison of SIFT injector flanges and $H_3^+ + N$ revisited. *Int. J. Mass Spectrom.* 202:351–61
82. Scott GBI, Milligan DB, Fairley DA, Freeman CG, McEwan MJ. 2000. A selected ion flow tube study of the reactions of small $C_mH_n^+$ ions with O atoms. *J. Chem. Phys.* 112:4959–65
83. Scott GBI, Fairley DA, Milligan DB, Freeman CG, McEwan MJ. 1999. Gas phase reactions of some positive ions with atomic and molecular oxygen and nitric oxide at 300 K. *J. Phys. Chem. A* 103:7470–73
84. Milligan DB, McEwan MJ. 2000. $H_3^+ + O$: an experimental study. *Chem. Phys. Lett.* 319:482–85
85. Barckholtz C, Snow TP, Bierbaum VM. 2001. Reactions of C_n^- and C_nH^- with atomic and molecular hydrogen. *Ap. J.* 547:L171–74
86. Tulej M, Kirkwood DA, Pachkov M, Maier JP. 1998. Gas-phase electronic transitions of carbon chain anions coinciding with diffuse interstellar bands. *Ap. J.* 506:L69–L73
87. Morris RA, Viggiano AA, Paulson JF. 1994. Electron detachment reactions of fluorinated carbanions with atomic hydrogen. *J. Chem. Phys.* 100:1767–68
88. Midey AJ, Viggiano AA. 2007. Kinetics of sulfur oxide, sulfur fluoride, and sulfur oxyfluoride anions with atomic species at 298 and 500 K. *J. Phys. Chem. A* 111:1852–59
89. Midey AJ, Miller TM, Morris RA, Viggiano AA. 2005. Reactions of $PO_xCl_y^-$ ions with H and H_2 from 298 to 500 K. *J. Phys. Chem. A* 109:2559–63

90. Eichelberger BR, Snow TP, Barckholtz C, Bierbaum VM. 2007. Reactions of H, N, and O atoms with carbon chain anions of interstellar interest: an experimental study. *Ap. J.* 667:1283–89
91. Poutsma JC, Midey AJ, Viggiano AA. 2006. Absolute rate coefficients for the reactions of $O_2^- + N(^4S_{3/2})$ and $O_2^- + O(^3P)$ at 298 K in a selected-ion flow tube instrument. *J. Chem. Phys.* 124:074301
92. Poutsma JC, Midey AJ, Thompson TH, Viggiano AA. 2006. Absolute rate coefficients and branching percentages for the reactions of $PO_xCl_y^- + N(^4S_{3/2})$ and $PO_xCl_y^- + O(^3P)$ at 298 K in a selected-ion flow tube instrument. *J. Phys. Chem. A* 110:11315–19
93. Eichelberger BR, Snow TP, Bierbaum VM. 2003. Collision rate constants for polarizable ions. *J. Am. Soc. Mass Spectrom.* 14:501–5
94. Scott GBI, Fairley DA, Freeman CG, McEwan MJ. 1997. The reaction $H_3^+ + N$: a laboratory measurement. *Chem. Phys. Lett.* 269:88–92
95. Fehsenfeld FC, Howard CJ, Ferguson EE. 1973. Thermal energy reactions of negative ions with H atoms in the gas phase. *J. Chem. Phys.* 58:5841–42